

Targeted disruption of the *Hexa* gene results in mice with biochemical and pathologic features of Tay–Sachs disease

(animal model/G_{M2} gangliosidosis/homologous recombination/lysosomal storage disease)

SHOJI YAMANAKA*, MARK D. JOHNSON†, ALEX GRINBERG†, HEINER WESTPHAL†, JACQUELINE N. CRAWLEY‡, MASAKO TANIKE§, KINUKO SUZUKI§, AND RICHARD L. PROIA*¶

*Section on Biochemical Genetics, Genetics and Biochemistry Branch, National Institute of Diabetes and Digestive and Kidney Diseases, †Laboratory of Mammalian Genes and Development, National Institute of Child Health and Development, ‡Section on Behavioral Neuropharmacology, Experimental Therapeutics Branch, National Institute of Mental Health, National Institutes of Health, Bethesda, MD 20892; and §Department of Pathology, University of North Carolina, Chapel Hill, NC 27599-7525

Communicated by Ernest Beutler, June 22, 1994

ABSTRACT Tay–Sachs disease, the prototype of the G_{M2} gangliosidoses, is a catastrophic neurodegenerative disorder of infancy. The disease is caused by mutations in the *HEXA* gene resulting in an absence of the lysosomal enzyme, β -hexosaminidase A. As a consequence of the enzyme deficiency, G_{M2} ganglioside accumulates progressively, beginning early in fetal life, to excessive amounts in the central nervous system. Rapid mental and motor deterioration starting in the first year of life leads to death by 2–4 years of age. Through the targeted disruption of the mouse *Hexa* gene in embryonic stem cells, we have produced mice with biochemical and neuropathologic features of Tay–Sachs disease. The mutant mice displayed <1% of normal β -hexosaminidase A activity and accumulated G_{M2} ganglioside in their central nervous system in an age-dependent manner. The accumulated ganglioside was stored in neurons as membranous cytoplasmic bodies characteristically found in the neurons of Tay–Sachs disease patients. At 3–5 months of age, the mutant mice showed no apparent defects in motor or memory function. These β -hexosaminidase A-deficient mice should be useful for devising strategies to introduce functional enzyme and genes into the central nervous system. This model may also be valuable for studying the biochemical and pathologic changes occurring during the course of the disease.

Tay–Sachs disease is a fatal neurodegenerative disorder of infancy inherited in an autosomal recessive fashion (for review, see ref. 1). Affected infants, by the age of 3–5 months, show signs of motor weakness and decreasing attentiveness. Mental and motor deterioration progresses rapidly leading to a completely unresponsive state and, by age 2–4 years, a fatal outcome. Tay–Sachs disease results from a deficiency of the A (acidic) isozyme of lysosomal β -hexosaminidase (EC 3.2.1.52), a heterodimer of α and β subunits. Mutations in the *HEXA* gene, which encodes the α subunit of β -hexosaminidase, cause the A isozyme deficiency. The B (basic) isozyme, a β -subunit dimer, is present at normal or elevated levels in patients. Only the A isozyme, however, has the capacity to degrade G_{M2} ganglioside in concert with the G_{M2} activator, a ganglioside binding protein. In the absence of the A isozyme, G_{M2} ganglioside accumulates in neurons beginning in fetal life. The ganglioside is stored in the form of concentrically arranged lamellae known as membranous cytoplasmic bodies (MCBs). By the terminal stage of Tay–Sachs disease, most neurons have ballooned with MCBs filling their cytoplasm and distorting cellular architecture.

Tay–Sachs disease is the prototype of a group of disorders, the G_{M2} gangliosidoses, characterized by defective G_{M2} gan-

glioside degradation. In addition to mutations in the *HEXA* gene, mutations in the *HEXB* gene, encoding the β subunit of β -hexosaminidase, and in the G_{M2} activator gene also impair G_{M2} ganglioside degradation. Defects in the *HEXB* gene and in the G_{M2} activator gene cause Sandhoff disease and the AB variant of G_{M2} gangliosidosis, respectively. Disorders of lesser severity and later-onset occur when mutations in the *HEXA* or *HEXB* gene result in partial enzyme deficiency.

There is no effective therapy for Tay–Sachs disease or for other lysosomal storage disorders with central nervous system (CNS) involvement. Potential approaches include enzyme replacement (2) and gene transfer therapy (3). However, evaluation of these therapeutic strategies will require suitable animal models. Although well-characterized feline models of Sandhoff disease have been described (4, 5), no model of Tay–Sachs disease exists. With the goal of creating an animal model for Tay–Sachs disease, we have produced mice totally deficient in β -hexosaminidase A through disruption of the mouse *Hexa* gene by homologous recombination (6, 7).

MATERIALS AND METHODS

Targeting Vector Construction. First a plasmid was constructed containing both the neomycin-resistance (Neo) gene and the herpes simplex virus thymidine kinase (TK) gene. The expression cassette of pMC1NeopolyA (6) (Stratagene) was excised with *Xho* I and *Sal* I and inserted into the *Sal* I site of the pBluescript KS vector. The TK gene was placed under the control of the mouse phosphoglycerate kinase gene promoter and cloned into the *Kpn* I site in the opposite orientation from the Neo gene. Genomic clones from a 129/sv strain library (Stratagene; catalogue 946306) containing the mouse *Hexa* gene were isolated and characterized as described (8). A 7-kb genomic fragment, inclusive of exons 2–7 and a portion of exon 8, was cloned into the *Xho* I site between the TK and Neo genes. Next, a 3-kb fragment containing the remainder of exon 8 and exons 9–13 was inserted into the *Sal* I and *Hind*III sites downstream of the Neo gene. The organization of the targeting construct is illustrated in Fig. 1a.

Selection of Targeted Embryonic Stem (ES) Cells and Generation of Mutant Mice. The targeting vector (50 μ g) was linearized with *Hind*III endonuclease and introduced into the

Abbreviations: ES, embryonic stem; MCB, membranous cytoplasmic body; MU-GlcNAc, 4-methylumbelliferyl-2-acetamido-2-deoxy- β -D-glucopyranoside; MU-GlcNAc-6-SO₄, 4-methylumbelliferyl-6-sulfo-2-acetamido-2-deoxy- β -D-glucopyranoside; Neo, neomycin resistance; TK, thymidine kinase; CNS, central nervous system; PAS, periodic acid-Schiff.

¶To whom reprint requests should be addressed at: Building 10, Room 9D-15, National Institutes of Health, Bethesda, MD 20892.

The publication costs of this article were defrayed in part by page charge payment. This article must therefore be hereby marked "advertisement" in accordance with 18 U.S.C. §1734 solely to indicate this fact.

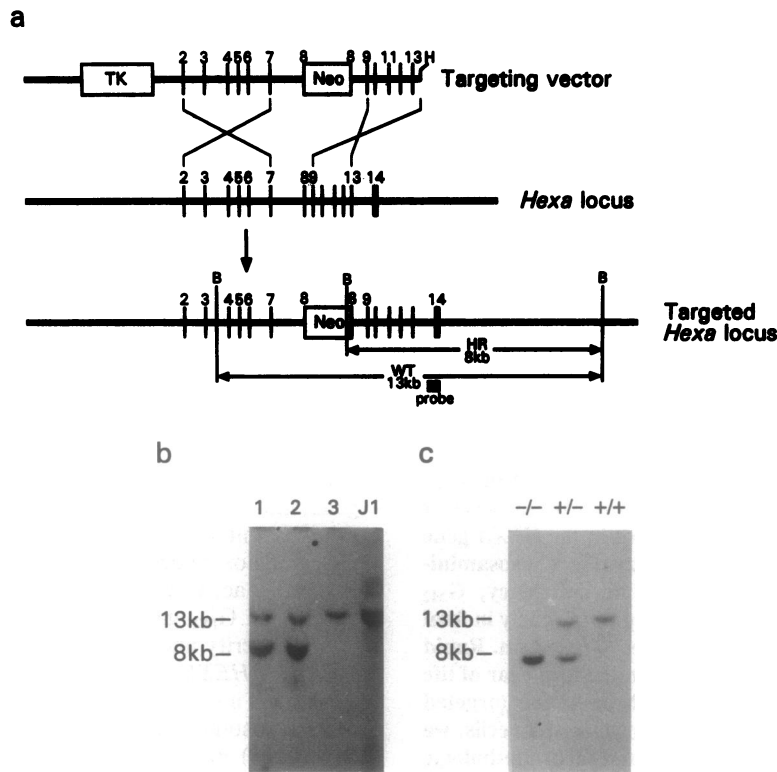


FIG. 1. Targeted disruption of the *Hexa* locus. (a) The structure of the mouse *Hexa* targeting vector is indicated on top, the *Hexa* locus is in the middle, and the predicted structure of the homologously recombined locus is on the bottom. (b) Southern blot analysis of targeted ES clones. Genomic DNA was isolated, digested with *Bam*HI endonuclease, electrophoresed on a 1% agarose gel, and transferred to GeneScreenPlus membranes. The hybridization probe is shown in a. Lanes 1 and 2 show correctly targeted clones. Lane 3 shows a G418-resistant clone that had not undergone homologous recombination. Lane 4 shows the parental J1 line. (c) Southern blot analysis of tail DNA from *Hexa* +/+, +/-, and -/- mice. The conditions for Southern blot analysis were as described above.

J1 line of ES cells (2.5×10^7 cells) by electroporation (400 V and 25 μ F) in a Bio-Rad Gene Pulser. The ES cells were plated on 20 100-mm plates containing mitomycin C-treated mouse embryonic fibroblast feeder layers in HEPES-buffered (20 mM, pH 7.3) high glucose Dulbecco's modified Eagle's medium (GIBCO) supplemented with 15% (vol/vol) fetal bovine serum (Hyclone), 0.1 mM nonessential amino acids (GIBCO), 0.1 mM 2-mercaptoethanol, murine leukemia inhibitory factor (GIBCO; 1000 units/ml), penicillin (50 units/ml) and streptomycin (50 μ g/ml). After 36 hr, the cells were placed under selective conditions in the medium described above containing G418 [GIBCO; 350 μ g/ml (dry weight)] and 5 μ M ganciclovir. After 8 days, colonies were picked, dispersed with trypsin into 15-mm plates, and grown for 3–4 days. The cells were transferred into 60-mm plates, and after 3–4 days, a portion of the cells was frozen and a portion was used to isolate DNA for Southern blot analysis.

ES cells from targeted lines TS-25 and TS-58 were injected into the blastocoel cavity of 3.5-day C57BL/6 embryos. Chimeric mice were bred to C57BL/6 females and the agouti offspring were tested for transmission of the disrupted allele by Southern blot analysis. Homozygous mutant mice were obtained by heterozygous matings.

β -Hexosaminidase Assays. Extracts of liver were prepared in 10 mM sodium phosphate (pH 6.0) containing 100 mM NaCl and 0.1% Triton X-100 and were loaded on a Mono Q column using the FPLC (Pharmacia). After washing with 5 ml of the loading buffer, the column was developed with 10 ml of a NaCl gradient from 100 mM to 400 mM NaCl. Fractions were assayed for β -hexosaminidase activity with 4-methylumbelliferyl-2-acetamido-2-deoxy- β -D-glucopyranoside (MU-GlcNAc) and 4-methylumbelliferyl-6-sulfo-2-acetamido-2-deoxy- β -D-glucopyranoside (MU-GlcNAc-6-SO₄) (Sigma) (9).

Pathology. Mice were anesthetized and briefly perfused through the left cardiac ventricle with heparinized saline and then with appropriate fixatives.

For routine light microscope study, mice were perfused with 4% (wt/vol) paraformaldehyde. Paraffin-embedded sections (6 μ m thick) were stained with hematoxylin/eosin or Luxol fast blue/periodic acid-Schiff (PAS) stains.

For electron microscopic analysis, tissues were fixed with either glutaraldehyde and paraformaldehyde or glutaraldehyde alone, dehydrated, and embedded in Epoxy resin (Polyscience). Sections 1 μ m thick were cut and stained with toluidine blue. Ultrathin sections were double stained with uranyl acetate and lead citrate and examined with an electron microscope (Zeiss 10A).

Immunocytochemistry was performed on frozen sections using chicken anti-G_{M2} ganglioside antibody (Matreya, Pleasant Gap, PA) and peroxidase-conjugated rabbit affinity-purified antibody to chicken IgG. The details will be published elsewhere, but are available from the authors upon request.

Behavioral Methods. All procedures were conducted in accordance with the National Institutes of Health Guide for the Care and Use of Laboratory Animals and approved by the National Institute of Mental Health Animal Care and Use Committee. *Hexa* -/- mice (five females and four males) and *Hexa* +/- mice (four females and four males) were 3–5 months of age at the time of behavioral testing.

Mice were individually tested for motor coordination and balance on a standard Rotorod apparatus (10), set at 4 rpm.

Individual mice were tested for spontaneous exploratory locomotion in a standard Digiscan open field, equipped with horizontal and vertical photocells to detect movements and with a microprocessor data analyzer (Omnitech Electronics, Columbus, OH) (11, 12).

Mice were individually tested for memory function in a mouse shuttlebox (ENV-101M; MED Associates, Lafayette, IN) equally divided into a lighted transparent compartment and a dark compartment (10, 13). On the training day, the mouse was placed into the lighted compartment, and 10 sec later the door between the compartments was raised. As soon as the mouse entered the dark compartment, the door was closed and a single foot shock was administered (0.3 mA for 1-sec duration). Ten seconds later, the mouse was returned to the home cage. Twenty-four hours later, the test consisted of placing the mouse in the lighted compartment, opening the door 10 sec later, and recording the time until the mouse completely entered the dark compartment (latency to enter, in seconds).

Analysis of variance was conducted to compare genotype and gender on behavioral parameters. Newman-Keuls post hoc test was conducted after a significant analysis of variance to determine which groups were different.

RESULTS

Targeted Disruption of the Mouse *Hexa* Gene. To disrupt the *Hexa* gene in mouse ES cells, a replacement-type targeting vector (6) was created with a 10-kb genomic segment isolated from a 129/sv strain library (Fig. 1a). Earlier attempts at gene targeting using smaller nonisogenic vectors were unsuccessful. The MC1NeopolyA cassette was inserted into exon 8 of the 14-exon *Hexa* gene (8) to disrupt the gene and to allow positive selection of cells integrating the vector. Additionally, the TK gene was placed in a position flanking the homologous sequences to enable selection against nonhomologous integrants. The linearized targeting vector was introduced into the J1 ES cell line by electroporation and the cells were cultured in the presence of G418 and ganciclovir. The ganciclovir selection resulted in an apparent 2.4-fold enrichment of homologous integrants. Genomic DNA from G418- and ganciclovir-resistant colonies was examined by Southern blot analysis using a hybridization probe from outside the region contained within the targeting vector (Fig. 1b). Of the 76 colonies examined in this manner, 9 exhibited the 8-kb *Bam*HI fragment illustrative of the homologously recombined allele in addition to the 13-kb fragment denoting the wild-type allele. Cells from two targeted ES clones, TS25 and TS58, were injected into the blastocoel cavity of 3.5-day C57BL/6 embryos and were transplanted into foster mothers. With both cell lines, highly chimeric mice were obtained that readily transmitted the mutant allele to their offspring. The heterozygotes were intercrossed to obtain mice homozygous for the disrupted gene (Fig. 1c). Identical results were obtained with *Hexa* $-/-$ mice derived from cell lines TS25 and TS58.

The Targeted Disruption of the *Hexa* Gene Results in a Null Allele. Hexosaminidase exists as both A (acidic) and B (basic) isozymes that are separable by ion-exchange chromatography in both mice and humans (14). Only β -hexosaminidase A can effectively hydrolyze the sulfated substrate MU-GlcNAc-6-SO₄, due to the presence of the α subunit (15). A liver homogenate from *Hexa* $+/+$ mice, after chromatography on a Mono Q column, demonstrated two fractions of β -hexosaminidase activity (Fig. 2A). The nonadherent fraction corresponded to β -hexosaminidase B and hydrolyzed the neutral substrate MU-GlcNAc but not the sulfated substrate MU-GlcNAc-6-SO₄. The adherent fraction corresponded to β -hexosaminidase A and hydrolyzed both the sulfated and neutral substrates. Liver extracts from *Hexa* $-/-$ mice displayed abundant β -hexosaminidase B with <1% of normal β -hexosaminidase A activity (Fig. 2C). The enzyme profile from *Hexa* $+/-$ mice indicated intermediate levels of β -hexosaminidase A relative to β -hexosaminidase B (Fig. 2B).

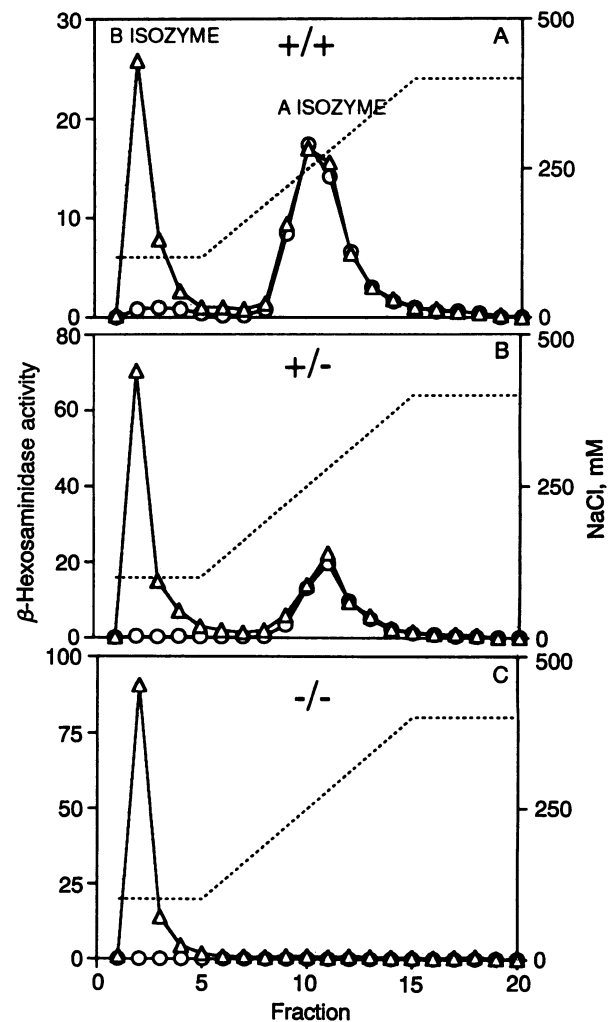


Fig. 2. *Hexa* $-/-$ mice are totally deficient in β -hexosaminidase A activity. Liver extracts from *Hexa* $+/+$ (A), $+/-$ (B), or $-/-$ (C) mice were subjected to ion-exchange chromatography on a Mono Q column. The fractions collected were assayed for β -hexosaminidase activity (nmol of substrate cleaved per hr) with either MU-GlcNAc (Δ) or MU-GlcNAc-6-SO₄ (\circ). The NaCl concentration gradient is indicated by the dotted line.

Liver RNA from *Hexa* $+/+$, *Hexa* $+/-$, and *Hexa* $-/-$ animals was examined by Northern blot analysis (Fig. 3). A *Hexa* transcript of 2.1 kb was present in liver RNA from *Hexa* $+/+$ and *Hexa* $+/-$ mice. Neither the 2.1-kb nor any other size transcript related to *Hexa* was apparent in liver RNA from *Hexa* $-/-$ mice. Densitometry of the blot revealed that the level of hybridizing material in the lane containing *Hexa* $-/-$ RNA was <2% of the wild type after normalization to β -actin levels. To eliminate the possibility that skipping of the disrupted exon during RNA splicing may have occurred in the *Hexa* $-/-$ mice, we performed reverse transcription of RNA followed by PCR amplification with primers flanking the site of Neo insertion. A 1.4-kb *Hexa* fragment containing the majority of the coding region was detected with *Hexa* $+/+$ RNA. No fragment was detected with *Hexa* $-/-$ RNA. Less than 0.5% of the wild-type amount of *Hexa* RNA could be detected under these conditions (data not shown).

***Hexa* $-/-$ Mice Progressively Accumulate G_{M2} Ganglioside.** The ganglioside fraction was isolated from brains of *Hexa* $-/-$ and *Hexa* $+/-$ mice and was analyzed by high-performance thin layer chromatography (Fig. 4). In 1-day-old *Hexa* $-/-$ mice, a faint band corresponding to G_{M2} ganglioside was barely detectable (<3% of total ganglioside).

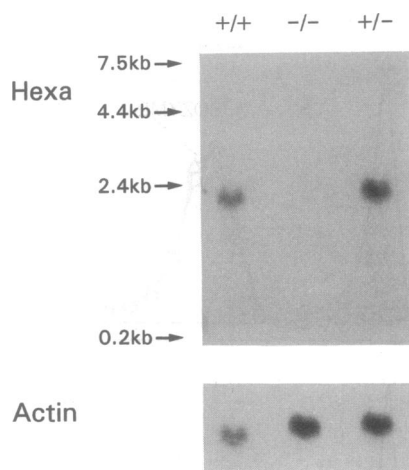


FIG. 3. *Hexa*^{-/-} mice are deficient in *Hexa* mRNA. Total RNA was isolated from livers of *Hexa*^{+/+}, *Hexa*^{+/-}, and *Hexa*^{-/-} mice and was examined by Northern blot analysis. (Upper) The hybridization was performed with a ³²P-labeled *Hexa* cDNA probe. (Lower) The membrane was stripped and rehybridized with a ³²P-labeled human actin cDNA.

The amount of G_{M2} ganglioside progressively increased in the brains of 1-month- and 6-month-old animals, representing 8.5 and 15% of total ganglioside, respectively. G_{M2} ganglioside was not detectable in brains from *Hexa*^{+/-} mice.

***Hexa*^{-/-} Mice Display Neuropathology Characteristic of Tay-Sachs Disease.** Pathologic examination was carried out on mice ranging in age from 7 weeks to 8 months. In light microscopic sections of cerebral cortex in the youngest mice, only rare neurons with vacuolated perikarya containing fine Luxol fast blue-positive granules within vacuoles were detected (data not shown). In Epoxy-resin-embedded sections (1 μm), identification of cortical neurons with MCBs was enhanced (Fig. 5A). With advancing age, numbers of storage neurons containing MCBs increased. On frozen sections, storage neurons were identified by the presence of strongly PAS-positive granules in their perikarya. The distribution of neurons containing PAS-positive granules, indicative of those with MCBs, corresponded with neurons immunostained with an antibody directed against G_{M2} ganglioside (Fig. 5B). There were no PAS-positive or immunoreactive neurons or MCBs in control brains (data not shown). At the ultrastructural level, these MCBs displayed concentrically arranged lamellae identical to the structures described in Tay-Sachs disease (Fig. 5C) (17). Unlike the terminal stage of Tay-Sachs disease in which practically all neurons are affected, however, the distribution of storage neurons in mice appeared to be localized in certain regions. In the cerebrum

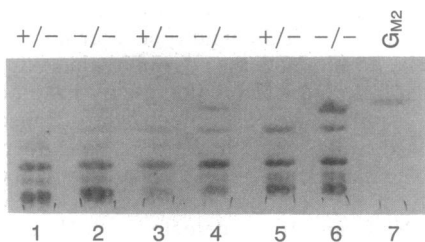


FIG. 4. G_{M2} ganglioside accumulates with time in the brains of *Hexa*^{-/-} mice. The ganglioside fraction was isolated (16) from the brains of *Hexa*^{+/-} and *Hexa*^{-/-} mice, as indicated, at the ages of 1 day (lanes 1 and 2), 4 weeks (lanes 3 and 4), 8 months (lane 5), and 6 months (lane 6). The G_{M2} standard is in lane 7. The gangliosides were resolved by thin-layer chromatography using silica gel 60 high-performance thin layer chromatography plates and visualized by spraying with the resorcinol hydrochloride reagent (16).

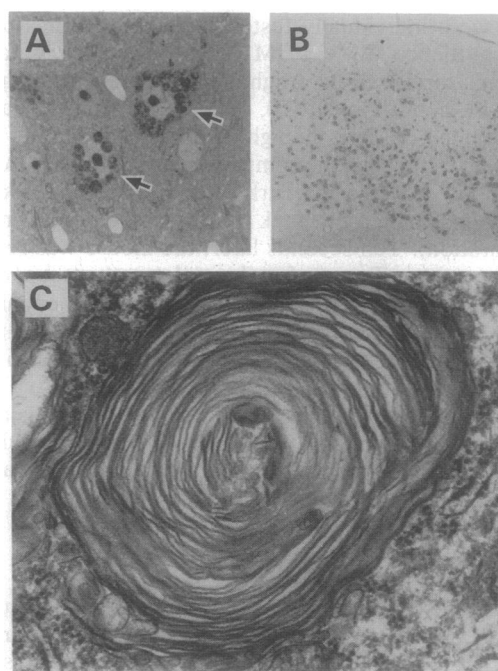


FIG. 5. *Hexa*^{-/-} mice show the neuropathology characteristic of Tay-Sachs disease. (A) MCBs are clearly recognized in the perikarya of two neurons in the parietal cortex from a *Hexa*^{-/-} mouse. A 1-μm Epoxy resin section was stained with toluidine blue. (×330.) (B) Many neurons are immunostained with anti-G_{M2} ganglioside antibody in a 7-μm cryosection of the mamillary body from an 8-month-old mouse. Note the dark peroxidase reaction product staining the neurons. Sections from control mice were totally negative for the reaction product. (×30.) (C) Electron micrograph of an MCB composed of multilayered lamellae in a cerebral cortical neuron from a 7-week-old *Hexa*^{-/-} mouse. (×9500.)

of 8-month-old mice, storage neurons were well recognized in the cerebral cortex and, in particular, the piriform and entorhinal cortices, Ammons horn (CA3), amygdala, mamillary bodies, septal nuclei, and nuclei in the hypothalamus. They were also noted in some regions of the brain stem. They were absent in the olfactory bulb and the cerebellar cortex. In the spinal cord, rare storage neurons were seen in the posterior horn. There were no obvious storage cells in the heart, lung, thymus, liver, spleen, lymph nodes, pancreas, adrenal gland, kidney, and reproductive organs. A few neurons containing MCBs were noted within the myenteric plexus.

***Hexa*^{-/-} Mice Are Viable and Have Not Shown Neurologic Disturbances.** Heterozygous matings yielded *Hexa*^{-/-} progeny in the frequency expected from Mendelian genetics, suggesting that homozygosity for the disrupted *Hexa* allele does not cause embryonic lethality. *Hexa*^{-/-} mice grow normally and have survived for >12 months. Both males and females are fertile and can be bred to each other.

Hexa^{-/-} mice, aged 3–5 months, were tested to determine whether abnormal neurologic manifestations were present (Table 1). The mutant mice exhibited normal balance and motor behavior when tested on a standard Rotorod apparatus (10). The mice were also subjected to an open field exploratory test to monitor sedation, hyperactivity, ataxia, or other gross behavioral abnormalities (11, 12). No significant differences between *Hexa*^{+/-} and *Hexa*^{-/-} mice were observed in any of the parameters measured. The passive-avoidance task was used as an initial test for deficits in learning and memory (10, 13). No significant differences were detected between genotypes for the latency to enter a dark compartment 24 hr after receiving a foot shock in that location.

Table 1. *In vivo* analysis of *Hexa* genotypes

Parameter	+/- female	-/- female	+/- male	-/- male
Body weight, g	19.4 ± 1.1	19.5 ± 1.1	28.2 ± 0.8	28.4 ± 1.2
Rotorod (latency to fall), sec	>60	>60	>60	>60
Horizontal activity, movements per 5 min	1282 ± 158	1122 ± 37	1369 ± 109	1201 ± 114
Passive avoidance (latency to enter), sec	121 ± 60	122 ± 60	146 ± 53	108 ± 68

Values are the mean ± SEM.

DISCUSSION

Mice homozygous for the disrupted *Hexa* locus exhibit the underlying defect in Tay–Sachs disease, a complete absence of the A isozyme of β -hexosaminidase. The B isozyme was present differentiating this model from the feline models of G_{M2} gangliosidosis where both the A and B isozymes were absent due to mutation in the feline equivalent of the *HEXB* gene. As a consequence of the β -hexosaminidase A deficiency, G_{M2} ganglioside accumulates in the CNS of the *Hexa* -/- mice in an age-dependent fashion. The G_{M2} ganglioside accumulation resulted in storage neurons with staining properties and intraneuronal inclusions (MCBs) that were identical to affected neurons in Tay–Sachs disease patients (1, 17). Consistent with the progressive accumulation of G_{M2} ganglioside, the numbers of storage neurons increased with age.

Unlike Tay–Sachs disease patients, in which, ultimately, all neurons are affected, certain regions of the nervous system in the *Hexa* -/- mice were spared or showed limited ganglioside storage. No neuronal storage was found in the cerebellum, the anterior horn of the spinal cord, or the spinal ganglia. Only minor storage was present in the posterior horn of the spinal cord. A possible explanation for this disparity may be differences in the metabolic pathway of G_{M2} ganglioside in humans and mice. In this regard, Burg *et al.* (18) had reported evidence suggesting β -hexosaminidase B may have G_{M2} ganglioside degrading activity in the mouse. Although our results demonstrate an essential role for β -hexosaminidase A in G_{M2} ganglioside degradation in mice, even a very low rate of ganglioside degradation by β -hexosaminidase B could dramatically alter the progression of the disease. The consequences of a low level of residual enzyme activity is seen in late-onset G_{M2} gangliosidosis patients who exhibit >5% of normal activity (19). In contrast to Tay–Sachs disease, in the late-onset disorder the ganglioside storage is much less pronounced and displays a restricted pattern of accumulation in the brain (20). The late-onset form is also clinically milder with less conspicuous neurological manifestations compared to Tay–Sachs disease.

A second possibility, not exclusive of the first, is that the very large difference in the gestational time of mice and humans could result in a disparity in the extent of ganglioside storage present at birth. Neuronal ganglioside accumulation begins very early in human fetal development in Tay–Sachs disease. In a study of CNS pathology in Tay–Sachs disease during the fetal period, abnormal inclusions were present in some neurons of the anterior horn of the spinal cord at 12 weeks, the earliest time examined (21). At 18–20 weeks of gestation, G_{M2} ganglioside levels in the brain were already increased 4- to 5-fold in brain (22). Newborn *Hexa* -/- mice, after their 3-week gestational period, show very little G_{M2} ganglioside with significant accumulation occurring thereafter. As a result, the *Hexa* -/- mice may mirror a very early stage of the human disease.

The onset of neurological symptoms in Tay–Sachs disease patients occurs by 3–5 months after birth (1). We have not detected any abnormal neurologic signs in the *Hexa* -/- mice by that age. Their normal motor coordination and

exploratory locomotion were consistent with the lack of neuronal storage in the anterior horn of the spinal cord and cerebellum. The pronounced storage in the hippocampus and entorhinal cortex suggested that memory function might be impaired in the *Hexa* -/- mice. However, no difference was found in the results of the passive-avoidance memory task between mice homozygous and heterozygous for the disrupted *Hexa* allele. This negative finding may indicate that a more sophisticated memory task is necessary or that the level of ganglioside accumulation at 3–5 months of age is insufficient to impair the hippocampal and cortical functions involved in learning and memory.

The *Hexa* -/- mice with their CNS ganglioside storage and attendant neuropathology will be useful for studies on the efficacy of functional enzyme replacement and gene therapy in lysosomal storage diseases with CNS involvement. The model should also be valuable to study the progression of biochemical and morphological changes that occur during the disease process.

We are grateful to Kunihiko Suzuki for helpful discussions and to Peggy Hsieh and Debra Boles for their comments on the manuscript. We thank Evelyn Grollman for help with the ganglioside analysis, Olivia Johnson for help in preparing the targeting vector, Teresa Bone-Turrentine and Clarita Langemann for preparation of light and electron microscope sections, Carol Markey for assistance with the behavioral experiments, and Linda Robinson for secretarial assistance. We also thank En Li and Rudolf Jaenisch for the J1 cells. This work was supported in part by U.S. Public Health Service Grants NS-24453 and HD03110 (K.S.).

- Sandhoff, K., Conzelmann, E., Neufeld, E. F., Kaback, M. M. & Suzuki, K. (1989) in *The Metabolic Basis of Inherited Disease*, eds. Scriver, C. R., Beaudet, A. L., Sly, W. S. & Valle, D. (McGraw-Hill, New York), Vol. 2, pp. 1807–1839.
- Dobrenis, K., Joseph, A. & Rattazzi, M. C. (1992) *Proc. Natl. Acad. Sci. USA* **89**, 2297–2301.
- Suhr, S. T. & Gage, F. H. (1993) *Arch. Neurol.* **50**, 1252–1268.
- Cork, L. C., Munnell, J. F. & Lorenz, M. D. (1977) *Science* **196**, 1014–1017.
- Neuwelt, E. A., Johnson, W. G., Blank, N. K., Pagel, M. A., Masien-McClure, C., McClure, M. J. & Wu, P. M. (1985) *J. Clin. Invest.* **76**, 482–490.
- Capecchi, M. R. (1989) *Science* **244**, 1288–1292.
- Koller, B. H. & Smithies, O. (1992) *Annu. Rev. Immunol.* **10**, 705–730.
- Yamanaka, S., Johnson, O. N., Norflus, F., Boles, D. J. & Proia, R. L. (1994) *Genomics* **21**, 588–596.
- Kaback, M. M. (1972) *Methods Enzymol.* **28**, 862–867.
- Mathis, C., Paul, S. M. & Crawley, J. N. (1994) *Psychopharmacology*, in press.
- DeFries, J. C., Gervais, M. C. & Thomas, E. A. (1978) *Behav. Genet.* **8**, 3–13.
- Crawley, J. N. (1992) *J. Neurosci.* **12**, 3380–3391.
- Decker, M. W. & McGaugh, J. L. (1989) *Brain Res.* **477**, 29–37.
- Beccari, T., Orlacchio, A. & Stirling, J. L. (1988) *Biochem. J.* **252**, 617–620.
- Kytzia, H.-J. & Sandhoff, K. (1985) *J. Biol. Chem.* **260**, 7568–7572.
- Ledeer, R. W. & Yu, R. K. (1982) *Methods Enzymol.* **83**, 139–191.
- Terry, R. D. & Weiss, M. (1963) *J. Neuropathol. Exp. Neurol.* **22**, 18–55.
- Burg, J., Banerjee, A., Conzelmann, E. & Sandhoff, K. (1983) *Hoppe-Seyler's Z. Physiol. Chem.* **364**, 821–829.
- Conzelmann, E. & Sandhoff, K. (1991) *Dev. Neurosci.* **13**, 197–204.
- Suzuki, K. (1991) *Dev. Neurosci.* **13**, 205–210.
- Adachi, M., Schneck, L. & Volk, B. W. (1974) *Lab. Invest.* **30**, 102–112.
- Conzelmann, E., Nehrorn, H., Kytzia, H. J., Sandhoff, K., Macek, M., Lehovsky, M., Elleder, M., Jirasek, A. & Kobilkova, J. (1985) *Pediatr. Res.* **19**, 1220–1224.